Communication: Quasiclassical trajectory calculations of correlated product-state distributions for the dissociation of $(H_2O)_2$ and $(D_2O)_2$

Gábor Czakó,[a] Yimin Wang, and Joel M. Bowman
Cherry L. Emerson Center for Scientific Computation and Department of Chemistry, Emory University, Atlanta, Georgia 30322, USA

(Received 30 August 2011; accepted 4 October 2011; published online 18 October 2011)

Stimulated by recent experiments [B. E. Rocher-Casterline, L. C. Ch'ng, A. K. Mollner, and H. Reisler, J. Chem. Phys. **134**, 211101 (2011)], we report quasiclassical trajectory calculations of the dissociation dynamics of the water dimer, $(H_2O)_2$ (and also $(D_2O)_2$) using a full-dimensional *ab initio* potential energy surface. The dissociation is initiated by exciting the H-bonded OH(OD)-stretch, as done experimentally for $(H_2O)_2$. Normal mode analysis of the fragment pairs is done and the correlated vibrational populations are obtained by (a) standard histogram binning (HB), (b) harmonic normal-mode energy-based Gaussian binning (GB), and (c) a modified version of (b) using accurate vibrational energies obtained in the Cartesian space. We show that HB allows opening quantum mechanically closed states, whereas GB, especially via (c), gives physically correct results. Dissociation of both $(H_2O)_2$ and $(D_2O)_2$ mainly produces either fragment in the bending excited (010) state. The $H_2O(J)$ and $D_2O(J)$ rotational distributions are similar, peaking at $J = 3$–5. The computations do not show significant difference between the ro-vibrational distributions of the donor and acceptor fragments. Diffusion Monte Carlo computations are performed for $(D_2O)_2$ providing an accurate zero-point energy of 7247 cm^{-1}, and thus, a benchmark D_0 of 1244 ± 5 cm^{-1}.
 [doi:10.1063/1.3655564]

During the past decade, experimental techniques have been developed to measure correlated final state distributions in polyatomic chemical reactions, thereby tracking the energy flow along the reaction coordinate. For example, Liu and coworkers[1] have played a pioneering role in measuring correlated vibrational distributions of the HX + CH_3 products from the X + CH_4 reactions, where X = O, F, and Cl. Very recently, there have been a number of experimental studies of the internal state distributions of fragments of hydrogen bonded dimers;[2–5] and these are of particular relevance to the present work. Velocity map imaging techniques have been used to determine correlated product-state distributions and dissociation energies (D_0) of single-H-bonded dimers such as HCl-H_2O (Ref. 2), NH_3-H_2O (Ref. 3), $(H_2O)_2$ (Ref. 4), and $(NH_3)_2$ (Ref. 5). A recent experiment for $(H_2O)_2$ provided an accurate D_0 of 1105 ± 10 cm^{-1} (Ref. 4), which is in excellent agreement with a previous theoretical prediction of 1103 cm^{-1} obtained by utilizing diffusion Monte Carlo (DMC) simulations on an *ab initio* potential energy surface (PES).[6] In the experimental work, the bound OH-stretch (3601 cm^{-1}) was excited by one quantum resulting in the dissociation of the dimer. The experiment found that one of the fragment pairs was predominantly bending excited; however, experiment could not distinguish between donor and acceptor fragments.[4] A similar measurement for $(D_2O)_2$ is a "work in progress."[7] Recent experiments on NH_3-H_2O and $(NH_3)_2$ also found significant energy transfer into the (umbrella) bending mode of the NH_3 fragment(s) and reported accurate D_0 values of 1538 ± 10 and 660 ± 20 cm^{-1}, respectively.[3,5]

In the present communication, we report quasiclassical trajectory (QCT) calculations of the dissociation dynamics of $(H_2O)_2$ and $(D_2O)_2$. The QCT simulation of the correlated product-state distributions provides a significant challenge to theory, since quantum mechanically only a few vibrational states are energetically open. Therefore, we investigate different techniques to compute these distributions and show how one can overcome the unphysical energy redistribution issue of QCT.

We also take the same DMC approach used for $(H_2O)_2$ to compute a benchmark D_0 and zero-point energy (ZPE) for $(D_2O)_2$. These ZPEs are used to assess the accuracy of the harmonic ZPEs used in the trajectory calculations, and so, we discuss them next.

D_0 of $(D_2O)_2$: We performed DMC calculations for $(D_2O)_2$ using an *ab initio* full-dimensional PES, denoted as HBB2.[6] Gaussian random walkers were propagated by a "birth-death" process and the total number of walkers is kept approximately constant by adjusting the reference energy, E_{ref}, at every imaginary time step, τ, according to

$$E_{ref} = \langle V \rangle - \alpha \frac{N(\tau) - N(0)}{N(0)}, \quad (1)$$

where α equals 0.1 and $N(0)$ equals 20 000 in the present calculations. The ZPE is then estimated by averaging E_{ref} over 80 000 steps after an equilibrium stage of 2000 steps with a time step of 10 a.u. The initial distributions of walkers in the present calculations are delta functions centered at either the global minimum or the lowest first-order saddle point of the water dimer. The fully anharmonic ZPE of $(D_2O)_2$ obtained from this DMC calculation is 7247 cm^{-1}.

[a]Electronic mail: czako@chem.elte.hu.

Considering the D_e (1741 cm^{-1}) (Ref. 6) and the variationally computed ZPE of D_2O (3375 cm^{-1}) corresponding to the HBB2 PES, one obtains a new benchmark D_0 value of 1244 cm^{-1} for $(D_2O)_2$. Our rigorous calculation of D_0 validates a previous theoretical prediction of 1241 cm^{-1}, which was based on a rigid monomer model.[8] (The present D_0 value has an estimated systematic uncertainty of ± 5 cm^{-1}, due to systematic uncertainties in the dimer and monomer ZPEs.) The harmonic normal-mode ZPE is 7373 cm^{-1} for $(D_2O)_2$, whereas the accurate DMC value is 7247 cm^{-1} on the same PES. For $(H_2O)_2$, the fully anharmonic ZPE from DMC calculations is 9872 cm^{-1} and the harmonic result is 10 107 cm^{-1}.[6] Thus, the harmonic ZPEs are higher than the rigorous ones by 235 and 126 cm^{-1} for $(H_2O)_2$ and $(D_2O)_2$, respectively. Based on the harmonic ZPEs, one obtains D_0 values of 1008 and 1190 cm^{-1} for $(H_2O)_2$ and $(D_2O)_2$, respectively; thus, the corresponding harmonic approximations underestimate the D_0s by 95 and 54 cm^{-1}. More discussion of these differences and especially the determination of the vibrational energy of the fragments are given below.

Quasiclassical trajectory calculations: We have performed QCT simulations for the dissociation of $(H_2O)_2(v_{OH} = 1)$ and $(D_2O)_2(v_{OD} = 1)$ using the HBB2 PES.[6] Standard normal mode sampling was applied to prepare the initial quasiclassical states by giving harmonic ZPE for each mode and an extra quantum of excitation to the bound OH or OD stretching fundamental, i.e., almost a local mode of the donor denoted as v_{OH} or v_{OD}. The total rotational angular momentum of the dimers was set to zero. A total of 10 000 trajectories for each dimer were propagated for about 25 ps using 0.25 fs time steps. The product states of the fragments were analyzed for the dissociated trajectories, where the final O-O distance is larger than 10 Å. After 25 ps, about 84% and 25% of the $(H_2O)_2$ and $(D_2O)_2$ trajectories dissociated, respectively. QCTs predict that the half life of $(H_2O)_2(v_{OH} = 1)$ is about 13 ps and several times longer for $(D_2O)_2(v_{OD} = 1)$. Note that QCT may underestimate the lifetimes due to the "ZPE leak," as was investigated for the isomerizations of the water trimer in Ref. 9. Since the mode-specific product-state assignment for the polyatomic products as well as the "binning" of these states plays a central role in the present simulation, we briefly describe the techniques employed and their advantages and limitations.

Product-state analysis and binning techniques: First, we remove the classical angular momentum using standard modification to the velocities in the Cartesian space resulting in $\mathbf{v}_i^{nr}$ ($i = 1, 2, \ldots, N$) for an N-atomic molecule. Second, we relate the final product configuration, with Cartesian coordinates denoted by $\mathbf{r}_i$ ($i = 1, 2, \ldots, N$), to normal mode displacements of a reference minimum geometry (denoted as $\mathbf{r}_i^{eq}$). The reference configuration is located by either a gradient-based optimization method starting from $\mathbf{r}_i$ or by finding the best overlap between $\mathbf{r}_i$ and a known equilibrium structure in the Cartesian space as described in Refs. 10 and 11, respectively. Having determined the relevant reference geometry, we perform a normal mode analysis there, which provides the harmonic frequencies ω_k, and the orthogonal transformation matrix, which transforms from mass-scaled Cartesian coordinates to normal coordinates. Thus, the normal coordinates (Q_k) and momenta (P_k) can be obtained by linear transformations from $\Delta\mathbf{r}_i = \mathbf{r}_i - \mathbf{r}_i^{eq}$ and $\mathbf{v}_i^{nr}$, respectively. By employing P_k and Q_k, the harmonic classical vibrational energy for each normal mode can be calculated. Thus, a non-integer classical harmonic action number (n'_k) for each mode can be obtained by the energy formula of a quantum harmonic oscillator. Finally, the integer vibrational quantum number is assigned by rounding n'_k to the nearest integer value n_k. Hereafter, we denote a vibrational state ($n_1, n_2, \ldots, n_{3N-6}$) as $\mathbf{n}$. The detailed description of the above procedure, including equations, is given in Ref. 10.

In order to get the probability of a particular vibrational state **n,** one can use either the widely used histogram binning (HB) or Gaussian binning (GB).[10,12–14] The HB gives that the probability of the state $\mathbf{n}$ is

$$P_{HB}(\mathbf{n}) = \frac{N(\mathbf{n})}{N_{traj}}, \tag{2}$$

where $N(\mathbf{n})$ is the number of products in state $\mathbf{n}$ from the total number of trajectories N_{traj}. A well-known issue of HB is that $P_{HB}(\mathbf{n})$ can be non-zero for an energetically closed state. When one uses GB, a Gaussian weight, $G_p(\mathbf{n})$, is calculated for each product, where $p = 1, 2, \ldots, N(\mathbf{n})$, and the probability of $\mathbf{n}$ can be obtained as

$$P_{GB}(\mathbf{n}) = \frac{\sum_{p=1}^{N(\mathbf{n})} G_p(\mathbf{n})}{\sum_{\mathbf{n}} \sum_{p=1}^{N(\mathbf{n})} G_p(\mathbf{n})}. \tag{3}$$

(Note that the normalization, shown in the denominator of Eq. (3), applies for unimolecular processes. This can be problematic for bimolecular reactions, where non-reactive trajectories exist; therefore, weights cannot be straightforwardly assigned to all the trajectories.) The application of GB for polyatomic products provides a considerable challenge, since $G_p(\mathbf{n})$ is the product of $3N-6$ weights, since one Gaussian weight can be assigned to each mode. Therefore, this extension of GB to polyatomic systems is computationally not feasible, because in a typical application, it requires 10^{3N-6} times more trajectories than HB in order to get the same statistical accuracy. In the present water dimer study, we have two triatomic products, i.e., six modes altogether, which would increase the computational time by a factor of roughly 10^6. In 2009, we proposed another strategy,[10] where the weight is obtained based on the total vibrational energy as

$$G_p(\mathbf{n}) = \frac{\beta}{\sqrt{\pi}} e^{-\beta^2\left(\frac{E(\mathbf{n}'_p)-E(\mathbf{n})}{2E(\mathbf{0})}\right)^2} \quad p = 1, 2, \ldots, N(\mathbf{n}), \tag{4}$$

where $\beta = 2\sqrt{\ln 2}/\delta$, δ is the full-width at half-maximum, $E(\mathbf{0})$ is the harmonic ZPE, and

$$E(\mathbf{n}'_p) = \sum_{k=1}^{3N-6} \omega_k \left(n'_{k,p} + \frac{1}{2}\right), \tag{5}$$

TABLE I. Normalized correlated vibrational product distributions for the dissociation of the water dimer.

	$(H_2O)_2(v_{OH}=1) \rightarrow H_2O(n_1n_2n_3)_d + H_2O(n_1n_2n_3)_a$				$(D_2O)_2(v_{OD}=1) \rightarrow D_2O(n_1n_2n_3)_d + D_2O(n_1n_2n_3)_a$			
$(n_1n_2n_3)_d + (n_1n_2n_3)_a$	ω[a]	HB[b]	GB(ho)[c]	GB(aho)[d]	ω[a]	HB[b]	GB(ho)[c]	GB(aho)[d]
$(000)_d + (000)_a$	9374	**0.07**	**0.07**	**0.04**	6822	**0.09**	**0.18**	**0.13**
$(000)_d + (010)_a$	1641	**0.07**	**0.26**	**0.43**	1201	**0.09**	**0.40**	**0.47**
$(010)_d + (000)_a$	1641	**0.07**	**0.24**	**0.46**	1201	**0.09**	**0.33**	**0.39**
$(000)_d + (020)_a$	3282	0.03	0.03	0.02	2402	0.06	0.02	0.00
$(020)_d + (000)_a$	3282	0.04	0.04	0.02	2402	0.07	0.01	0.00
$(010)_d + (010)_a$	3282	0.03	0.04	0.02	2402	0.06	0.01	0.00
$(000)_d + (100)_a$	3811	0.07	0.10	0.01	2747	0.05	0.02	0.00
$(100)_d + (000)_a$	3811	0.09	0.11	0.01	2747	0.08	0.01	0.00
$(000)_d + (001)_a$	3921	0.05	0.04	0.00	2873	0.04	0.01	0.00
$(001)_d + (000)_a$	3921	0.06	0.05	0.00	2873	0.05	0.02	0.00
Σ[e]		0.58	0.97	1.00		0.67	0.99	1.00

[a]Harmonic frequencies (in cm^{-1}) corresponding to the PES. The ω corresponding to $(000)_d + (000)_a$, where "d" and "a" refer to donor and acceptor, respectively, is the sum of the harmonic ZPEs of the monomers and all the other energies are relative to this ZPE.
[b]HB denotes standard histogram binning.
[c]GB(ho) denotes Gaussian binning based on the harmonic normal mode approximation [Eq. (5)].
[d]GB(aho) denotes Gaussian binning based on the exact vibrational energy in the Cartesian space [Eq. (7)].
[e]Total population of the vibrational states listed here. There are a lot of other classically open states, especially when HB is used, but each of them has small percentage (usually $\ll 1\%$). The bold numbers denote the probabilities of the quantum mechanically open states.

and

$$E(\mathbf{n}) = \sum_{k=1}^{3N-6} \omega_k \left(n_k + \frac{1}{2}\right). \tag{6}$$

This energy-based GB uses only *one* Gaussian for a polyatomic product, which reduces the computational cost significantly relative to the mode-based GB (the above-mentioned factor of 10^{3N-6} becomes only 10). In 2010, Bonnet and Espinosa-García[14] reported a detailed theoretical justification of this energy-based GB and named it 1GB for the reasons mentioned. This method assigns small weights for energetically closed states, since for a closed state, $E(\mathbf{n}'_p)$ is (usually much) less than $E(\mathbf{n})$, unless the harmonic normal mode approximation fails and seriously overestimates $E(\mathbf{n}'_p)$. This may happen at highly distorted configurations. Therefore, here, we propose a modification of 1GB, where $E(\mathbf{n}'_p)$ is determined exactly in the Cartesian space as

$$E(\mathbf{n}'_p) = \frac{1}{2}\sum_{i=1}^{N} m_i \mathbf{v}_{i,p}^{\mathrm{nr}} \left(\mathbf{v}_{i,p}^{\mathrm{nr}}\right)^{\mathrm{T}} + V(\mathbf{r}_{1,p}, \mathbf{r}_{2,p}, \ldots, \mathbf{r}_{N,p}) - V\left(\mathbf{r}_1^{\mathrm{eq}}, \mathbf{r}_2^{\mathrm{eq}}, \ldots, \mathbf{r}_N^{\mathrm{eq}}\right), \tag{7}$$

where $\mathbf{v}_{i,p}^{\mathrm{nr}}$ is the velocity of the pth product corresponding to zero classical angular momentum, m_i is the mass of the ith atom, and V is the potential energy of the N-atomic molecule.

Product-state distributions for the dissociation of the water dimer: We determined the normal-mode quantum numbers for the water fragment pairs using the procedure described above. The correlated vibrational populations, obtained by HB, 1GB with Eq. (5), and 1GB with Eq. (7), are given in Table I. Note that in the present implementation, 1GB means one Gaussian weight for each fragment; thus, the weight of a correlated state is the product of two Gaussians.

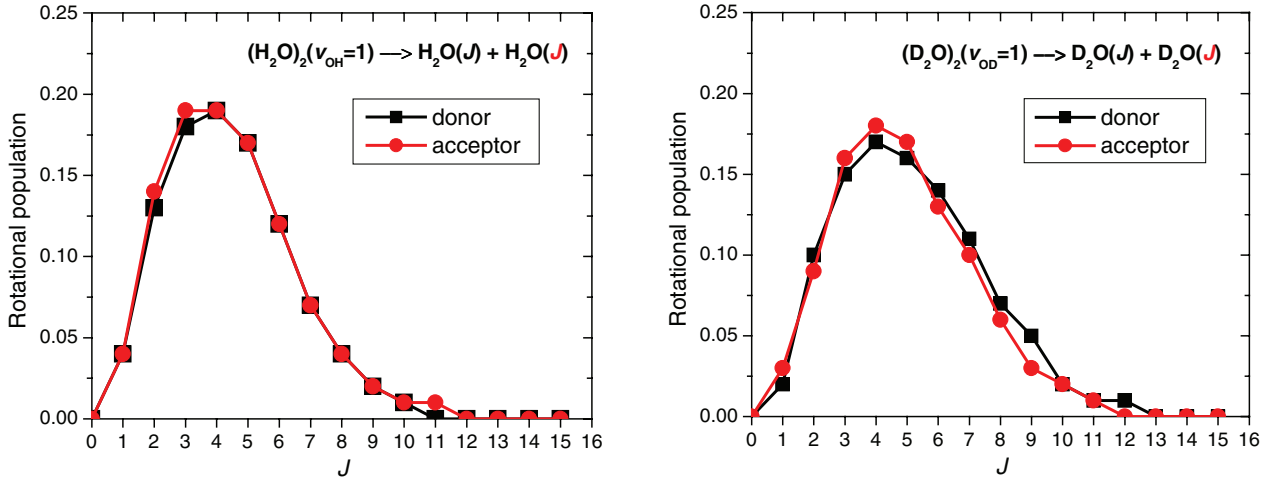

FIG. 1. Rotational distributions of the fragments obtained from the dissociation of the water dimer following the excitation of the bound OH/OD stretching fundamental.

Therefore, 1GB assigns small weights for trajectories in which either of the fragments violates ZPE, thereby effectively addressing the usual ZPE issue of the QCT method. Considering $v_{OH} - D_0[(H_2O)_2]$ and $v_{OD} - D_0[(D_2O)_2]$, the available energies for ro-vibrational excitation of the fragments are $3601 - 1103 = 2498$ cm^{-1} and $2632 - 1244 = 1388$ cm^{-1} for H_2O and D_2O, respectively. (Note that the harmonic approximation, used in QCT, provides higher available energies, i.e., $3734 - 1008 = 2726$ cm^{-1} and $2700 - 1190 = 1510$ cm^{-1}, respectively. The extra 228 and 122 cm^{-1} energies may cause more internal excitations of the products, but these numbers are still small relative to the total energies in the QCT calculations, i.e., roughly 15 000 and 10 000 cm^{-1}, respectively.) Therefore, in both cases, only three correlated product states are energetically open, i.e., $(000)_d + (000)_a$, $(000)_d + (010)_a$, and $(010)_d + (000)_a$, where subscripts "d" and "a" denote the donor and acceptor fragments, respectively. As usual, (000) and (010) are the vibrational ground state and first-excited bending state of the water molecule, respectively. Table I shows that HB predicts non-zero probability to many states, including stretching excited states and bending overtones, which are energetically closed quantum mechanically. This clearly demonstrates the failure of HB for this application. GB improves the results significantly, especially when the exact classical expression [Eq. (7)] is used to calculate the actual vibrational energy. When the harmonic approximation is used in the normal mode space [Eq. (5)], GB has some issues especially for H_2O. Although we see significant improvement relative to HB, the population of some of the "closed" states even increased. We found that for excited states, when the kinetic energy part of the total vibrational energy is small and the potential is large, i.e., the geometry is highly displaced from equilibrium, Eq. (5) can seriously overestimate the actual molecular energy; thus, it allows assigning large weights for energetically closed states. When we use Eq. (7), the actual vibrational energy becomes correctly lesser than the assigned $E(\mathbf{n})$ for the stretching states and bending overtones, etc; thus, these energetically non-available states get small weights and their probabilities tend to zero. (Note that the Gaussians have finite widths, in the present case, $\delta = 0.1$; thus, GB can allow small non-zero weights for closed states.) As Table I shows using 1GB with Eq. (7), we get (almost) zero probabilities for all the states expected to be closed. Among the three open states, $(000)_d + (000)_a$ is the minor with 4% and 13% populations for H_2O and D_2O, respectively. 1GB shows that one of the fragments is usually bending excited and (010) can be either "d" or "a" without any significant preference. The significant population of (000) + (010) for $H_2O + H_2O$ is in qualitative agreement with experiment (as mentioned earlier, experiment cannot distinguish between "d" and "a").[4]

Figure 1 shows the rotational distributions for the fragments obtained by rounding the classical total angular momentum of each fragment to the nearest integer. The most populated H_2O rotational states are $J = 3$, 4, and 5. Note that in Ref. 4, these were the rotational states probed experimentally. The rotational distributions for the D_2O fragments are very similar to the H_2O ones, perhaps $D_2O(J)$ is slightly broader. The similar J distribution means that the rotational energy distribution for D_2O is significantly colder than that of H_2O. This is reasonable, since the available energy for internal excitation of the fragments is larger for H_2O than D_2O, i.e., 2498 and 1388 cm^{-1}, respectively, as mentioned above.

We also computed the distributions of the relative translational energies of the products. As expected, these distributions are cold for both the H_2O and D_2O fragment pairs showing peaks at zero and fast decays in the 0–500 cm^{-1} translational energy range. We plan to report a more detailed analysis of these distributions and their correlation to the ro-vibrational distributions in a future publication.

In summary, we determined a benchmark D_0 (1244 ± 5 cm^{-1}) for $(D_2O)_2$. Based on the experimentally verified high accuracy of the D_0 of $(H_2O)_2$,[4,6] the present prediction for $(D_2O)_2$ is expected to be accurate as well. We have demonstrated the utility of the energy-based Gaussian binning method and proposed a modification, which uses the exact vibrational energy obtained in the Cartesian space to calculate the weight. We advocate employing this binning method for quasiclassical product analysis of polyatomic systems.

We thank Hanna Reisler for discussions and the National Science Foundation (CHE-0848233) for financial support.

[1] J. J. Lin, J. Zhou, W. Shiu, and K. Liu, Science **300**, 966 (2003).
[2] B. E. Casterline, A. K. Mollner, L. C. Ch'ng, and H. Reisler, J. Phys. Chem. A **114**, 9774 (2010).
[3] A. K. Mollner, B. E. Casterline, L. C. Ch'ng, and H. Reisler, J. Phys. Chem. A **113**, 10174 (2009).
[4] B. E. Rocher-Casterline, L. C. Ch'ng, A. K. Mollner, and H. Reisler, J. Chem. Phys. **134**, 211101 (2011).
[5] A. S. Case, C. G. Heid, S. H. Kable, and F. F. Crim, J. Chem. Phys. **135**, 084312 (2011).
[6] A. Shank, Y. Wang, A. Kaledin, B. J. Braams, and J. M. Bowman, J. Chem. Phys. **130**, 144314 (2009).
[7] H. Reisler, personal communication (2011).
[8] W. Cencek, K. Szalewicz, C. Leforestier, R. van Harrevelt, and A. van der Avoird, Phys. Chem. Chem. Phys. **10**, 4716 (2008).
[9] G. Czakó, A. L. Kaledin, and J. M. Bowman, Chem. Phys. Lett. **500**, 217 (2010).
[10] G. Czakó and J. M. Bowman, J. Chem. Phys. **131**, 244302 (2009).
[11] G. Czakó, A. L. Kaledin, and J. M. Bowman, J. Chem. Phys. **132**, 164103 (2010).
[12] L. Bonnet and J. C. Rayez, Chem. Phys. Lett. **277**, 183 (1997).
[13] L. Bonnet and J. C. Rayez, Chem. Phys. Lett. **397**, 106 (2004).
[14] L. Bonnet and J. Espinosa-García, J. Chem. Phys. **133**, 164108 (2010).